Chemical Science

Accepted Manuscript

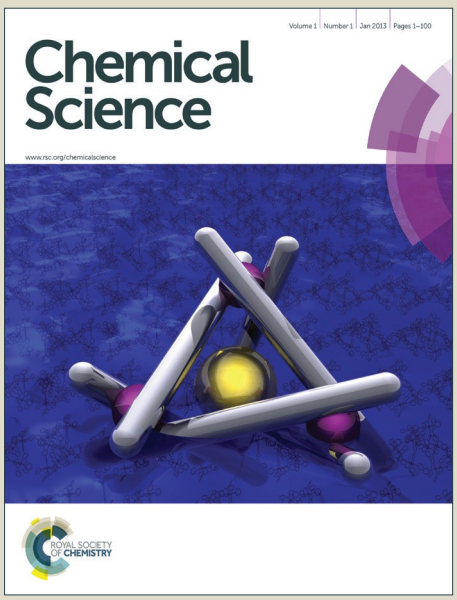

ROYAL SOCIETY OF CHEMISTRY

www.rsc.org/chemicalscience

Chemical Science

EDGE ARTICLE

Surfactants Encapsulated Palladium-Polyoxometalates: Controlled Assembly and Their Application as Single-atom Catalysts

Received 00th January 20xx,
Accepted 00th January 20xx

DOI: 10.1039/x0xx00000x

www.rsc.org/

Peilei He,[a] Biao Xu,[a] Xiaobin Xu,[a] Li Song,[b] and Xun Wang[a]

The challenge in the single-atom catalysts (SAC) is in designing a highly definite structure with accurate location of the single atom and high catalytic efficiency. The noble metal substituted polyoxometalates seem to be a kind of SAC because of their well resolved crystal structure. Here we got two kinds of assembly structures (nanoroll and hollow spindle) based on the palladium substituted Wells-Dawson polyoxometalate (Pd-POM) which consisted of isolated Pd atom. Both the nanorolls and hollow spindles showed high catalytic activity for both Suzuki-Miyaura coupling reaction and semihydrogenation reaction. The difference of chemical surroundings between the nanoroll and hollow spindle leads to their discrepancy in the catalytic activity of semihydrogenation.

Introduction

Supported metal catalyst as a kind of heterogeneous catalyst has been widely used in industry because of its higher catalytic efficiency. However, in the traditional supported noble metal catalyst, only a small portion of noble metal atoms act as the active center.[1] To improve the atom efficiency, single-atom catalysts (SAC) are the most promising catalyst which can decrease the use of noble metal and increase the catalytic efficiency to save energy.[2, 3, 4] In the recent advances, most of the single atoms were anchored to metal oxides,[5, 6] metal surface,[7] and graphene[8] in the SAC through mass-selected soft-landing technique[9] or wet chemistry method.[10] The single noble metal atoms on the supports can only be confirmed by the subangstrom-resolution scanning transmission electron microscopy (STEM).[11, 12] Even so, the location and coordination environment of the single atom is unpredictable in the catalyst.

How to get a SAC with accurate location and coordination environment of the noble metal is still a major challenge. Based on our understanding of polyoxometalates (POMs), we found that one noble metal atom can be incorporated into the POMs as heteroatom.[13] And the crystal structures of the noble metal substituted POMs are usually so well resolved. There are a series of noble metal substituted POM in the literature.[9] Therefore, this kind of POMs can be a good candidate of SACs with explicit component, structure and coordination environment. What's more, the structure diversity of POMs provides the chance to discover a new large class of SACs.

However, the direct use of pure polyoxometalate often associated with difficult catalyst recovery[14, 15] and lower efficiency in the organic catalytic reaction. A much simpler method is to encapsulate the POMs with surfactants.[16, 17] The surfactants encapsulated POMs (SEPs) are much easier to recovery and show better dispersibility in the organic solvent.[18, 19] Meanwhile, the chemical surrounding of POMs can be easily tuned based on the choice of surfactants. Especially, the surface properties of SEPs will be changed. So, through this method, numerous heterogeneous single atom catalysts could be got based on all kinds of POM.

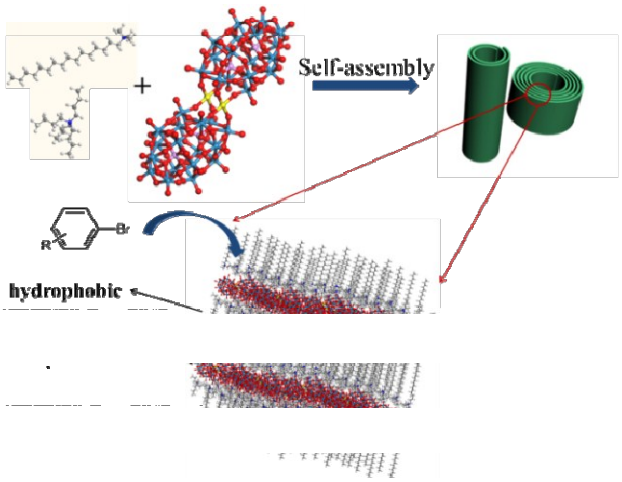

Figure 1. Schematic illustration of the Pd-POM nanoroll and the two kinds of catalytic reactions.

[a] Department of Chemistry, Tsinghua University, Beijing, 100084, China
E-mail: wangxun@mail.tsinghua.edu.cn
[b] National Synchrotron Radiation Laboratory, University of Science and Technology of China, Hefei, 230029, China
Electronic Supplementary Information (ESI) available. See DOI: 10.1039/x0xx00000x

Palladium Compounds are often used as catalyst in many organic reactions, such as coupling reaction,[20] hydrogenation,[21] and selective oxidation.[22] Therefore, in this work, we presents a nice study on controlled assembly of palladium substituted Wells-Dawson POM[23] (Pd-POM) with different surfactants and their application as single-atom catalysts. And these surfactants encapsulated Pd-POM could assemble into nanorolls and hollow spindles. When the Pd-POM was encapsulated by cetrimonium bromide (CTAB) and tetrabutylammonium bromide (TBAB), we observed some nanorolls with different length-diameter (L/D) ratio and coiling cycles (Figure 1). Some hollow spindles were obtained when the surfactants were decyltrimethylammonium bromide (DTAB) and tetraethylammonium bromide (TEAB). Most importantly, the as obtained assemblies could act as high-performance catalysts in both Suzuki-Miyaura coupling reactions and semi-hydrogenation of alkynes with TOF as high as above 2000 h^{-1} and stereo-selectivity of Z/E > 99/1. The current concept and results are very important and would be very enlightening in both materials science and catalysis fields.

Results and discussion

First, we have synthesized the Pd-POM ($K_{15}[Pd_2(\alpha_2\text{-}P_2W_{17}O_{61})_2H]$) according to the reference[23]. The structure of this kind Pd-POM can be confirmed by the ^{31}P NMR, mass spectrum and Fourier transform infrared (FTIR) characterization (Figure S1, S2). The chemical composition of Pd-POM was determined by inductively coupled plasma optical emission spectrometry (ICP-OES). And the experimental data (K, 6.359; P, 1.118; Pd, 2.631; W, 64.34) was very close to the calculated data (K, 6.426; P, 1.357; Pd, 2.332; W, 68.49). X-ray photoelectron spectrum (XPS) revealed that the valence state of Pd is +2 (Figure S3). Then a two-phase method[16] was used to get the SEPs. And we still employed two kinds of surfactants.[24, 25] When the surfactants were CTAB and TBAB, a yellow film (as Figure 2a shows) was observed after the evaporation of chloroform. Then the film was dissolved in the chloroform and some nanoroll structures occurred (Figure S4). After adjusting the volume ratio of chloroform and acetone to 2:1, the pure nanoroll structures were obtained as shown in Figure 2c and 2d. Then the pure nanoroll sample could be got when the organic solvent was completely evaporated. From the TEM image (Figure 2c), there were some nanorolls with different L/D ratios. The STEM result (Figure 2e) showed the structure of nanoroll much clearer. And some bundles of the nanorolls could be found. When some individual nanorolls were standing, cross-section could be easily observed. And we have investigated the nanorolls on small-angle X-ray diffraction (SAXRD) characterization. The interlayer spacing was about 2.8 nm (Figure 2f) which was corresponding to the result of HRTEM image (Figure 2d). The formation mechanism of the nanoroll should be the same with the mechanism we have discussed in the previous paper.[24] And the composition of nanorolls has been fully characterized by FTIR (Figure S5a), thermogravimetric analysis (TGA, Figure S5b) and C, H, N

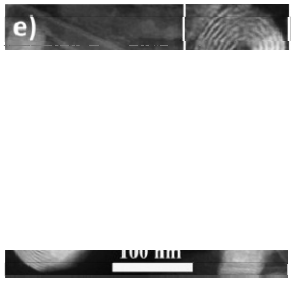

Figure 2. a) The photo image of the film which was composed of the nanorolls. Inset: static contact angle of the film. b) The photo image of the spindle powders. Inset: static contact of the spindle. c) TEM image of the nanorolls. Inset: the scheme of the nanorolls with different L/D ratio. d) HRTEM image of the nanorolls. e) STEM image of the nanorolls. Inset: a magnified image of a nanoroll. f) SAXRD of the nanorolls and hollow spindles.

elemental analysis (Figure S6). The TGA data indicated the full substitution of organic cations. The contact angle of the nanorolls was about 89 degree (the inset in Figure 2a) which was a little hydrophobic. When we used DTAB and TEAB, we got a hollow spindle structure (Figure S7) in the aqueous phase. The hollow spindle sample (Figure 2a) was got after the water was completely evaporated. The length of the hollow spindle was about 500 nm (Figure S7a). The lamellar structures have been observed in the magnified TEM image (Figure S7b) and has been confirmed by the SAXRD characterization (Figure 2f). The hollow structure was very obvious in the STEM image (Figure S7c). The contact angle of the spindle-like structure was about 5.4 degree (the inset in Figure 2b) caused by the decrease of chain length of the surfactants. The difference of the contact angle between the naroll and hollow spindle leads to the difference of the formation of film (Figure 2a) or precipitate (Figure 2b). The FTIR spectrum (Figure S8a) proved the existence of surfactants. Also, the TGA (Figure S8b) and C, H, N elemental analysis (Figure S6) have been done. Energy disperse X-ray (EDX) mapping (Figure S9) analysis of these two kinds of SACs confirmed the even distribution of nitrogen, phosphorous, tungsten and palladium.

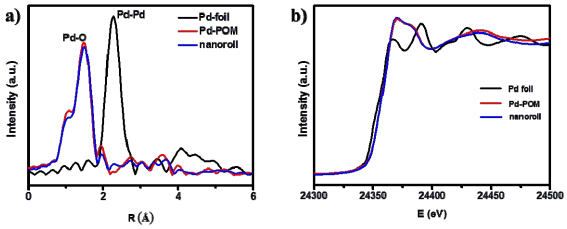

Figure 3. a) Fourier-transformed spectra of k^3-weighted Pd K-edge EXAFS of Pd foil, Pd-POM and nanoroll. b) The normalized XANES spectra at the Pd K-edge of Pd foil, Pd-POM and nanoroll.

To verify the Pd-POM contained only atomically dispersed single Pd atoms as the crystal structure shows (Figure 1), extended X-ray absorption fine structure (EXAFS) spectra was measured on the pure Pd-POM and nanoroll structure. Indeed, in the Fourier-transformed EXAFS spectra (r space, Figure 3a), there was only one peak at ~1.5 Å from the Pd-O contribution in the Pd-POM and no peak at ~2.26 Å from the Pd-Pd contribution. The EXAFS data did not reveal any Pd-Pd contribution in Pd-POM, in agreement with there was only Pd-O bond in the crystal structure. And the X-ray absorption near-edge structure (XANES) spectra of Pd-POM, nanoroll and the reference spectra of Pd foil were showed in Figure 3b. The whiteline intensities of Pd in the Pd-POM and nanoroll were almost exactly the same. Both of them were higer than the intensity of Pd foil. The whiteline intensity reflects the oxidation state of Pd in different sample.[26] So this result suggested that the Pd single atoms in Pd-POM carry positive charges. These results further proved the nanorolls and hollow spindles are SACs.

According to the reference,[27] the Pd^{2+} complexs are active in the Suzuki-Miyaura coupling reaction. Therefore, to test the catalytic activity of the SACs we got, Suzuki-Miyaura coupling reaction was selected as the model reaction. The Suzuki-Miyaura coupling reaction involves the coupling of an aryl halide (include iodide, bromide and chloride) and aromatic boronic acid. In general, aryl iodide is the most active substrate, and aryl chloride is the most inert. Meanwhile, it has been reported the room-temperature (RT) reaction between aryl bromide and phenylboronic acid.[28, 29] For this reason, we chose aryl bromide and RT to perform the Suzuki-miyaura coupling reaction. After optimizations, we selected C_2H_5OH-H_2O (1:1 mL) as the co-solvent, TBAB as the phase-transfer catalyst and K_2CO_3 as a base for the catalytic reaction. The amount of catalyst has been tested to determine the optimum reaction condition. And we found that 0.13 mol% Pd ($6.4*10^{-7}$ mole, combined with the ICP result, Figure S10) was sufficient for obtaining excellent yield of 4-acetylbiphenyl (96%, Table S1, entry 1) in 20 min, at 303K. The cross-coupling reaction was completed in 20 min, resulting in the Turnover Frequency (TOF) up to 2250 h^{-1}.

In order to see the catalytic efficiency of this catalytic system, a series of aryl halides were used as substrate to carry out the coupling reaction under optimized conditions (Table S1). High yield from 80% to 97% were obtained for different substrates. All the products were purified by column chromatography and verified by ^1H NMR and ^{13}C NMR (in the supporting information). Compared with 4-bromoanisole (Table S1, entry 5) and 4-bromoacetophenone (Table S1, entry 1), we could see the stronger the electron-donating group in aryl bromide was, the lower the catalytic activity was. Although the steric hindrance of 3-bromobenzaldehyde was increased, the decrease in yield was not obvious (Table S1, entry 13). The hollow spindles have also been taken to catalyze the Suzuki-Miyaura reaction. There might be a difference of chemical surroundings between the nanoroll and the hollow spindle structure according to their different contact angles. However, the hollow spindle structure showed similar catalytic activity to the nanoroll structure (Table S1). The main reason was that in the ethanol-water system we used both the nanoroll and hollow spindle structures have similar dispersibility and thus perform similar catalytic efficiency. Control experiments with $(CTA)_3(TBA)_3P_2W_{18}O_{62}$ and $(CTA)_x(TBA)_{(10-x)}P_2W_{17}O_{61}$ were also carried out under the same conditions. As reaction time was prolonged to 12 hours, there was still no coupling product. Therefore, the catalytic activity is the Pd atom in the SEPs.

The great advantage of the supported metal catalyst is the repeatable use of catalysts. Therefore, the recycle experiment has been achieved when catalyst is the nanoroll. The structure of Pd-POM could be maintained according to the FTIR and ^{31}P NMR characterization (Figure S11b and S11c), though the morphology of the nanorolls has changed after the catalytic reaction (Figure S11a). And the catalyst could be recycling for several times (Figure 4). There was an apparent loss of its high catalytic performance at the fourth cycle. Comparing the FTIR spectrum before and after the catalytic reaction, the apparent change was the decrease of the band at 2925 cm^{-1}. The band was corresponding to the methylene which was from the CTAB and TBAB. So we could speculate that the surfactants in SEP stripped from the surface of POM during the reaction. Considering TBAB was added into the reaction system, we have tried to add CTAB into the solution before the catalyst

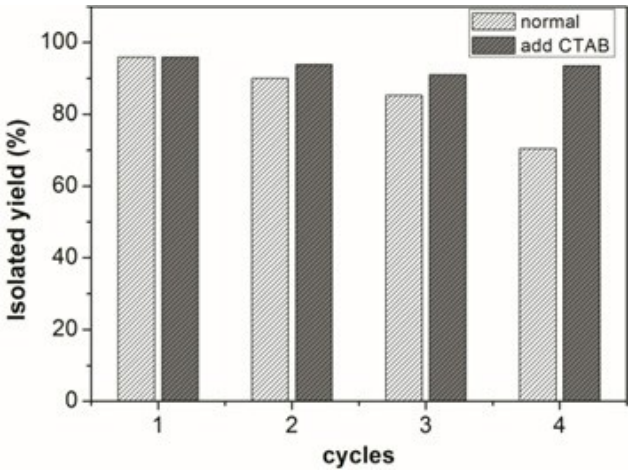

Figure 4. Catalytic experiment of recycled nanorolls for Suzuki-Miyaura Coupling reaction without or with addition of CTAB.

was reused. And we measured the loss of catalyst through weighing the mass of catalyst. As Figure S12 shows, the results indicate the loss of catalyst is more obvious without the addition of CTAB. Amazingly, the high catalytic performance can be kept after four cycles (Figure 4). In the control experiment, we have known that the yield of 4-bromoacetophenone with bare Pd-POM is 36% (entry 3, Table S1). It was much lower than the nanoroll or the hollow spindle structure. These results indicated the surfactants have positive effects on the Suzuki-Miyaura reaction. A more likely reason is that the aryl bromide and phenylboronic acid are organics. The hydrophobic alkyl chains of the surfactants on the surface of nanoroll and hollow spindle contributed to enhance the probability of the interaction between the organic reactants and the catalytic center (Pd-POM). Also, the surfactants can decrease the loss of Pd-POM in the aqueous solution. For the bare Pd-POM, there's no surfactant on the surface which is adverse to the contact between the reactants and the bare Pd-POM. Some previous reports about SEP-based reusable catalysts support our results.[30, 31]

Encouraged by the high activity of these SACs, we tried to examine their catalytic efficiency in other reactions. Pd compounds have also been studied for the semihydrogenation of alkynes with H_2 but suffer from lower Z-selectivity and over-reduction of alkenes.[32, 33] According to the reference,[34] they reported the highly selective semihydrogenation of alkynes by using organosilanes with water as a hydrogen source. Compared with hydrogen gas, organosilanes is a more promising hydrogen source because it's more prone to reaction under mild conditions. So we used the nanoroll and hollow spindle to catalyze semihydrogenation by using organosilanes as the hydrogen source. First, according to the reference,[22] we have known the solvent have a great effect on the catalytic activity. After screening of the solvents, we found chloroform as the only suitable solvent could afford high yield in the reaction. It was sufficient to use 0.15 mol% Pd for obtaining excellent yield of cis-stilbene (87%, Z/E > 99/1, Table 1, entry 1) in 30 min, at 298K. The nanoroll was further used to catalyze various internal alkynes under the same condition. For all these reactions, higher yield from 86% to 91% and higher stereoselectivity (Z/E > 99/1) were obtained. In this case, the Pd-POM could be seen as a kind of shape selective catalyst. As the Figure S13 shows, the reactant approached to the Pd atoms in semi-open space of the Pd-POM's center. The two Pd atoms located in the same side of reactant. Therefore, the hydrogenation reaction was more incline to happen on the one side of reactant. Finally, most of the semihydrogenation products were cis-form product. After the catalytic reaction, some nanodisks occurred instead of the nanorolls (Figure S14a). The structure of the Pd-POM kept unchanged according to FTIR spectra (Figure S14b) in spite of the change of morphology. In addition, the catalyst could be recycled by centrifugation and used for another cycle without obvious loss of the catalytic activity (Table 1, entry 5, in parentheses). Then the catalytic activity of the hollow spindle structure was also examined with different internal alkynes. Through Table 1, we can see the nanoroll shows much higher catalytic activity than

Table 1. The scope of the semihydrogenation reactions. [a]

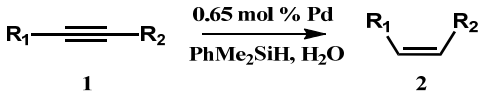

1 2

1a: $R_1 = C_6H_5$, $R_2 = C_6H_5$
1b: $R_1 = C_6H_5$, $R_2 = CO_2C_2H_5$
1c: $R_1 = n\text{-}C_6H_{13}$, $R_2 = CO_2CH_3$

Entry	Catalyst	1	Yield [%][b]	Z/E[c]
1	nanoroll	**1a**	87	>99/1
2	spindle	**1a**	37	>99/1
3	nanoroll	**1b**	87	>99/1
4	spindle	**1b**	12	>99/1
5[d]	nanoroll	**1c**	91 (90[e])	>99/1
6	spindle	**1c**	67	>99/1
7	Pd-POM	**1c**	64	>99/1

[a] Unless otherwise noted, the reactions were carried out with **1** (0.1mmol), dimethylphenylsilane (0.2mmol), and water (10 μL) in the presence of catalyst in $CHCl_3$ (2mL) at 25 °C for 30 min. [b] ^1H NMR yield, using CH_2Br_2 as an internal standard. [c] Z/E ratio was determined by 1H NMR analysis. [d] The reaction time was 15 min. [e] The yield of the second use. All the yield and Z/E ratio were in accordance with the GC-MS results.

the hollow spindle. In the control experiment (Table 1, entry 7), we have known that the catalytic activity of bare Pd-POM is similar to the hollow spindle. These apparent differences should be caused by the difference of chemical surroundings we have mentioned before. When the Pd-POM is encapsulated by CTAB and TBAB, the nanorolls show a comparatively large contact angle (89°) which leads them to disperse better in the organic solvents than the hydrophilic hollow spindles or the bare Pd-POM.

Besides, we carried out the leaching experiments to clarify whether the palladium leached into the reaction system (Figure S15). After 10 min (the yield is 23%), 1 mL of the reaction solution was filtered and the supernatant was transferred to another vessel. The supernatant and the residual reaction solution were continuously stirred for 20min. Though the yield of residue was 81%, the yield of supernatant was still 23%. These results indicate the semihydrogenation reaction is catalyzed by the solid catalyst.

Conclusions

In summary, we have found a new kind of SAC which was based on the palladium substituted polyoxometalates. Through the surfactant encapsulating process, some new assemblies, such as nanoroll and hollow spindle, have been obtained. Both of the nanoroll and hollow spindle showed impressively high catalytic activity for the Suzuki-Miyaura coupling reaction. The catalyst could be reused for several times without the loss of the high catalytic efficiency. In addition, the nanoroll could efficiently catalyze the semihydrogenation of alkynes with a higher Z-selectivity.

Moreover, we think the high efficiency of the single Pd atom in Pd-POM isn't limited to these two kinds of reaction. The single-atom catalyst with other noble metal in POM should be further studied.

Acknowledgements

This work was supported by NSFC (21431003, 91127040, 21221062), and the State Key Project of Fundamental Research for Nanoscience and Nanotechnology (2011CB932402)

References

1 X.-F. Yang, A. Wang, B. Qiao, J. Li, J. Liu and T. Zhang, *Acc. Chem. Res.*, 2013, **46**, 1740.
2 X. Guo, G. Fang, G. Li, H. Ma, H. Fan, L. Yu, C. Ma, X. Wu, D. Deng, M. Wei, D. Tan, R. Si, S. Zhang, J. Li, L. Sun, Z. Tang, X. Pan and X. Bao, *Science*, 2014, **344**, 616.
3 B. Qiao, A. Wang, X. Yang, L. F. Allard, Z. Jiang, Y. Cui, J. Liu, J. Li and T. Zhang, *Nat. Chem.*, 2011, **3**, 634.
4 Z.-J. Zhao, C.-c. Chiu and J. Gong, *Chem. Sci.*, 2015, **6**, 4403.
5 J. Lin, A. Wang, B. Qiao, X. Liu, X. Yang, X. Wang, J. Liang, J. Li, J. Liu and T. Zhang, *J. Am. Chem. Soc.*, 2013, **135**, 15314.
6 E. J. Peterson, A. T. DeLaRiva, S. Lin, R. S. Johnson, H. Guo, J. T. Miller, J. Hun Kwak, C. H. F. Peden, B. Kiefer, L. F. Allard, F. H. Ribeiro and A. K. Datye, *Nat Commun*, 2014, **5**, 4885.
7 M. Flytzani-Stephanopoulos and B. C. Gates, *Annu. Rev. Chem. Biomol. Eng.*, 2012, **3**, 545.
8 S. Sun, G. Zhang, N. Gauquelin, N. Chen, J. Zhou, S. Yang, W. Chen, X. Meng, D. Geng, M. N. Banis, R. Li, S. Ye, S. Knights, G. A. Botton, T.-K. Sham and X. Sun, *Sci. Rep.*, 2013, **3**, 1775.
9 U. Heiz, A. Sanchez, S. Abbet and W. D. Schneider, *J. Am. Chem. Soc.*, 1999, **121**, 3214.
10 H. Wei, X. Liu, A. Wang, L. Zhang, B. Qiao, X. Yang, Y. Huang, S. Miao, J. Liu and T. Zhang, *Nat Commun*, 2014, **5**, 5634.
11 A. Uzun, V. Ortalan, Y. Hao, N. D. Browning and B. C. Gates, *ACS Nano*, 2009, **3**, 3691.
12 A. A. Herzing, C. J. Kiely, A. F. Carley, P. Landon and G. J. Hutchings, *Science*, 2008, **321**, 1331.
13 N. V. Izarova, M. T. Pope and U. Kortz, *Angew. Chem. Int. Ed.*, 2012, **51**, 9492.
14 P. Yin, J. Wang, Z. Xiao, P. Wu, Y. Wei and T. Liu, *Chem. - Eur. J.*, 2012, **18**, 9174.
15 D. Huang, Y. J. Wang, L. M. Yang and G. S. Luo, *Ind. Eng. Chem. Res.*, 2006, **45**, 1880.
16 H. Li, H. Sun, W. Qi, M. Xu and L. Wu, *Angew. Chem. Int. Ed.*, 2007, **46**, 1300.
17 P. Yin, D. Li and T. Liu, *Isr. J. Chem.*, 2011, **51**, 191.
18 A. Nisar, Y. Lu, J. Zhuang and X. Wang, *Angew. Chem. Int. Ed.*, 2011, **50**, 3187.
19 A. Nisar, J. Zhuang and X. Wang, *Adv. Mater.*, 2011, **23**, 1130.
20 S.-W. Kim, M. Kim, W. Y. Lee and T. Hyeon, *J. Am. Chem. Soc.*, 2002, **124**, 7642.
21 D. Teschner, J. Borsodi, A. Wootsch, Z. Révay, M. Hävecker, A. Knop-Gericke, S. D. Jackson and R. Schlögl, *Science*, 2008, **320**, 86.
22 K. Mori, T. Hara, T. Mizugaki, K. Ebitani and K. Kaneda, *J. Am. Chem. Soc.*, 2004, **126**, 10657.
23 N. V. Izarova, A. Banerjee and U. Kortz, *Inorg. Chem.*, 2011 **50**, 10379.
24 P. He, B. Xu, H. Liu, S. He, F. Saleem and X. Wang, *Sci. Rep.*, 2013, **3**, 1833.
25 P. He, B. Xu, P.-p. Wang, H. Liu and X. Wang, *Adv. Mater.*, 2014, **26**, 4339.
26 J.-D. Grunwaldt, N. v. Vegten and A. Baiker, *Chem. Commun.*, 2007, DOI: 10.1039/B710222D, 4635.
27 M. Choi, D.-H. Lee, K. Na, B.-W. Yu and R. Ryoo, *Angew. Chem. Int. Ed.*, 2009, **48**, 3673.
28 B. Xu, H. Yang, G. Zhou and X. Wang, *Sci China Mater*, 2014 **57**, 34.
29 T. Maegawa, Y. Kitamura, S. Sako, T. Udzu, A. Sakurai, A. Tanaka, Y. Kobayashi, K. Endo, U. Bora, T. Kurita, A. Kozaki, Y. Monguchi and H. Sajiki, *Chem. - Eur. J.*, 2007, **13**, 5937.
30 L. Plault, A. Hauseler, S. Nlate, D. Astruc, J. Ruiz, S. Gatard and R. Neumann, *Angew. Chem. Int. Ed.*, 2004, **43**, 2924.
31 W. Qi, Y. Wang, W. Li and L. Wu, *Chem. - Eur. J.*, 2010, **16**, 1068.
32 J. Wu, K. J. Wang, Y. Li and P. Yu, *Adv. Mater. Res.*, 2011, **233**, 2109.
33 J. J. Brunet and P. Caubere, *J. Org. Chem.*, 1984, **49**, 4058.
34 M. Yan, T. Jin, Y. Ishikawa, T. Minato, T. Fujita, L.-Y. Chen, M. Bao, N. Asao, M.-W. Chen and Y. Yamamoto, *J. Am. Chem. Soc.*, 2012, **134**, 17536.